IV International Conference on Computational Methods for Coupled Problems in Science and Engineering
COUPLED PROBLEMS 2011
M. Papadrakakis, E. Oñate and B. Schrefler (Eds)

A SUBSTRUCTURING FE MODEL FOR STRUCTURAL-ACOUSTIC PROBLEMS WITH MODAL-BASED REDUCTION OF POROELASTIC INTERFACE

Romain Rumpler[*†], Jean-François Deü[*] and Peter Göransson[†]

[*]Structural Mechanics and Coupled Systems Laboratory (LMSSC)
Conservatoire National des Arts et Métiers
292 rue Saint-Martin, case 353, 75141 Paris Cedex 03, France
e-mail: deu@cnam.fr - www.cnam.fr/lmssc/

[†]The Marcus Wallenberg Laboratory for Sound and Vibration Research (MWL)
Department of Aeronautical and Vehicle Engineering, KTH
KTH School of Engineering Sciences, SE-100 44 Stockholm, Sweden
e-mail: pege@kth.se, rumpler@kth.se - www.kth.se/en/sci/institutioner/ave/avd/mwl

Key words: Poroelastic materials; Noise reduction; Reduced model; Structural-acoustics.

Abstract. In this work, a component mode synthesis technique is proposed to improve the computational efficiency of Finite Element problems including 3D modelling of poroelastic materials. The modal reduction relies on real-valued modes, solution of a standard eigenvalue problem, based on a classical solid and fluid displacements formulation of the porous media. Efficiency in terms of degrees of freedom, convergence, sparsity and computation time is presented.

1 INTRODUCTION

Modelling poroelastic materials for interior noise reduction, extensively used in the transport industry, can lead to rather expensive Finite Element (FE) models. Therefore, efforts have been made in the last decade to propose efficient solution strategies for the Biot-Allard theory [1]. Use of a mixed displacement-pressure formulation for the solid and fluid phases respectively [2] downsized the number of degrees of freedom (dofs) per node from 6, when using a standard solid and fluid phases displacement formulation, to 4 dofs. Hierarchical elements also proved to reduced the number of dofs needed to model the porous media [3]. The use of equivalent acoustic impedances [4, 5], while implying low computational cost, is limited by strong assumptions, or subject to a preliminary identification step thus hampering computational efficiency. Alternatively, modal reduction techniques have been proposed and applied to poroelastic FE formulations, in an attempt

to keep a fine and complex 3D modelling of the problem in the scope of low frequency applications [6–8].

In this work, a component mode synthesis is applied to the dissipative part of a 3D poro-acoustic FE problem. The standard solid and fluid displacements formulation is used to model poroelastic media. A direct computation scheme at each frequency increment is used to solve the frequency-dependent problem, and frequency response of the mean quadratic pressure in the acoustic domain is computed as an indicator of the sound level. Real-valued modes based on the bi-phase poroelastic media are used to define a transformation applied once at the initial increment, and suitable for the frequency range of interest. After a presentation of the formulation as well as the modal method used, the proposed reduction is tested on a rigid cavity treated with a porous layer on one wall. While showing substantial computation time speed-up, due to both the reduced number of dofs and the good sparsity of the reduced system, the relatively low convergence rate suggests further possible improvements.

2 FE FORMULATION FOR THE PORO-ACOUSTIC PROBLEM

A poro-acoustic problem is considered, which description and notations are presented on Fig. 1. The acoustic fluid and the porous media occupy the domains Ω_{F} and Ω_{P} respectively. The compressible fluid is described using pressure fluctuation (p) as primary variable (Subsection 2.1.1), while fluid and solid phases homogenized displacements ($\mathbf{u}_{\mathrm{s}}$,$\mathbf{u}_{\mathrm{f}}$) are retained as primary variables for the porous media (Subsection 2.1.2). The domains boundaries are separated into contours of:

- imposed Dirichlet boundary conditions denoted $\partial_1\Omega_{\mathrm{F}}$ and $\partial_1\Omega_{\mathrm{P}}$,
- prescribed Neumann boundary conditions denoted $\partial_2\Omega_{\mathrm{F}}$ and $\partial_2\Omega_{\mathrm{P}}$,
- coupling interface between acoustic fluid and porous media (Γ_{FP}).

The FE formulation is presented for a permanent harmonic response at angular frequency ω.

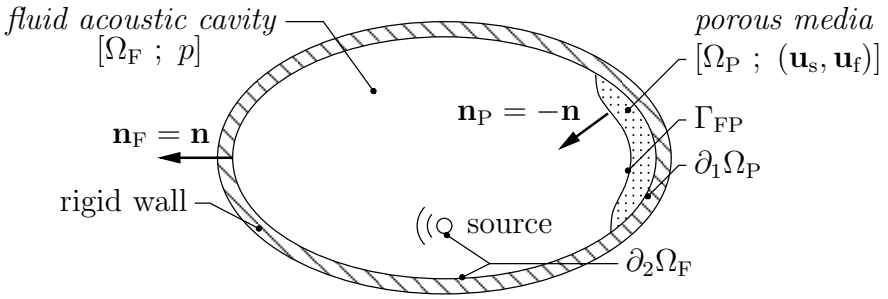

Figure 1: Description ans notations of the poro-acoustic interaction problem

2.1 Dynamic equations and constitutive laws

2.1.1 Compressible fluid (p)

The internal fluid within cavities is assumed compressible and inviscid, satisfying the Helmholtz equation derived from the motion, continuity, and constitutive equations:

$$\Delta p + \frac{\omega^2}{c_0^2} p = 0 \quad \text{in } \Omega_{\mathrm{F}} \tag{1}$$

where c_0 is the constant speed of sound in the fluid, and p the pressure fluctuation scalar field. The limit case $\omega = 0$ is not given by Equation (1). Though not considered in this work, the solution is given by the static solution of the coupled fluid-structure problem [9].

2.1.2 Porous media Biot theory ($\mathbf{u}_{\mathrm{s}}, \mathbf{u}_{\mathrm{f}}$)

Notation	Description
ρ_{s}	Solid frame density
$(\lambda;\, \mu)$	Lamé parameters for the solid frame
ρ_{f}	Ambient fluid density
η	Ambient fluid viscosity
P_0	Ambient fluid standard pressure
γ	Heat capacity ratio for the ambient fluid
Pr	Prandtl number for the ambient fluid
ϕ	Porosity
α_∞	Tortuosity
σ	Static flow resistivity
Λ	Viscous characteristic length
Λ'	Thermal characteristic length

Table 1: List of material parameters

At angular frequency ω, the poroelastic media satisfies the following elastodynamic linearized equations, derived in the Biot-Allard theory [1], taking into account inertia and viscous coupling effects between solid and fluid phases:

$$\operatorname{div} \boldsymbol{\sigma}_{\mathrm{s}} - \mathrm{i}\,\omega\, \widetilde{b}(\omega)(\mathbf{u}_{\mathrm{s}} - \mathbf{u}_{\mathrm{f}}) + \omega^2 \left[(\rho_{\mathrm{s}} + \rho_{\mathrm{a}})\mathbf{u}_{\mathrm{s}} - \rho_{\mathrm{a}}\mathbf{u}_{\mathrm{f}}\right] \quad = \mathbf{0} \quad \text{in } \Omega_{\mathrm{P}} \tag{2a}$$

$$\operatorname{div} \boldsymbol{\sigma}_{\mathrm{f}} - \mathrm{i}\,\omega\, \widetilde{b}(\omega)(\mathbf{u}_{\mathrm{f}} - \mathbf{u}_{\mathrm{s}}) + \omega^2 \left[-\rho_{\mathrm{a}}\mathbf{u}_{\mathrm{s}} + (\phi\rho_{\mathrm{f}} + \rho_{\mathrm{a}})\mathbf{u}_{\mathrm{f}}\right] = \mathbf{0} \quad \text{in } \Omega_{\mathrm{P}} \tag{2b}$$

where $\mathbf{u}_{\mathrm{s}}$ and $\mathbf{u}_{\mathrm{f}}$ are respectively the solid phase and fluid phase averaged displacements in the sense of Biot theory. $\widetilde{b}(\omega)$ (henceforth denoted $\widetilde{b}$, where $\widetilde{\ }$ refers to a complex-valued quantity) and ρ_{a} are respectively the complex frequency-dependent viscous drag and the inertia coupling parameter, based on the standard notations of material parameters introduced in Table 1 [1], and given by:

$$\widetilde{b} = \sigma\phi^2 \left[1 + \frac{4i\omega\alpha_\infty^2\eta\rho_{\mathrm{f}}}{\sigma^2\Lambda^2\phi^2}\right]^{\frac{1}{2}} \tag{3}$$

$$\rho_a = \phi \rho_\mathrm{f} \left(\alpha_\infty - 1\right) \tag{4}$$

$\boldsymbol{\sigma}_\mathrm{s}$ and $\boldsymbol{\sigma}_\mathrm{f}$ are the averaged stress tensors for the solid and fluid phases respectively. They satisfy the Lagrangian stress-strain relations developed by Biot:

$$\boldsymbol{\sigma}_\mathrm{s} = \left(\lambda + \frac{(1-\phi)^2}{\phi} \widetilde{K}_\mathrm{f}(\omega)\right) \mathrm{tr}\left[\boldsymbol{\varepsilon}(\mathbf{u}_\mathrm{s})\right] \mathbf{I} + 2\mu\, \boldsymbol{\varepsilon}(\mathbf{u}_\mathrm{s}) + (1-\phi)\, \widetilde{K}_\mathrm{f}(\omega)\, \mathrm{tr}\left[\boldsymbol{\varepsilon}(\mathbf{u}_\mathrm{f})\right] \mathbf{I} \tag{5a}$$

$$\boldsymbol{\sigma}_\mathrm{f} = (1-\phi)\, \widetilde{K}_\mathrm{f}(\omega)\, \mathrm{tr}\left[\boldsymbol{\varepsilon}(\mathbf{u}_\mathrm{s})\right] \mathbf{I} + \phi\, \widetilde{K}_\mathrm{f}(\omega)\, \mathrm{tr}\left[\boldsymbol{\varepsilon}(\mathbf{u}_\mathrm{f})\right] \mathbf{I} \tag{5b}$$

where $\boldsymbol{\varepsilon}(\mathbf{u}_\mathrm{s})$ and $\boldsymbol{\varepsilon}(\mathbf{u}_\mathrm{f})$ are the strain tensors associated to the averaged displacements vector fields $\mathbf{u}_\mathrm{s}$ and $\mathbf{u}_\mathrm{f}$, defined by:

$$\boldsymbol{\varepsilon}(\mathbf{v}) = \frac{1}{2}\left(\mathbf{grad}\, \mathbf{v} + \mathbf{grad}^T \mathbf{v}\right) \tag{6}$$

Beside the standard material parameters presented in Table 1, the effective bulk modulus of the fluid phase $\widetilde{K}_\mathrm{f}(\omega)$ (henceforth denoted $\widetilde{K}_\mathrm{f}$) is also introduced. For reasons to be presented in Subsection 3.2, its expression [1] is separated into its zero-frequency limit and complex frequency-dependent behaviour:

$$\widetilde{K}_\mathrm{f} = \frac{\gamma P_0}{\gamma - (\gamma - 1)\left[1 + \frac{8\eta}{i\omega Pr \Lambda'^2 \rho_\mathrm{f}} \left(1 + \frac{i\omega Pr \Lambda'^2 \rho_\mathrm{f}}{16\eta}\right)^{\frac{1}{2}}\right]^{-1}} = P_0 + \left(\widetilde{K}_\mathrm{f} - P_0\right) \tag{7}$$

which, when introduced in Equations (5), leads to the following expressions of the stress-strain relations using Voigt notation:

$$\boldsymbol{\sigma}_\mathrm{s} = \mathbf{D}_\mathrm{s}^{(1)}\, \boldsymbol{\varepsilon}(\mathbf{u}_\mathrm{s}) + \widetilde{\mathbf{D}}_\mathrm{s}^{(2)}(\omega)\, \boldsymbol{\varepsilon}(\mathbf{u}_\mathrm{s}) + \mathbf{D}_\mathrm{sf}^{(1)}\, \boldsymbol{\varepsilon}(\mathbf{u}_\mathrm{f}) + \widetilde{\mathbf{D}}_\mathrm{sf}^{(2)}(\omega)\, \boldsymbol{\varepsilon}(\mathbf{u}_\mathrm{f}) \tag{8a}$$

$$\boldsymbol{\sigma}_\mathrm{f} = \mathbf{D}_\mathrm{sf}^{(1)}\, \boldsymbol{\varepsilon}(\mathbf{u}_\mathrm{s}) + \widetilde{\mathbf{D}}_\mathrm{sf}^{(2)}(\omega)\, \boldsymbol{\varepsilon}(\mathbf{u}_\mathrm{s}) + \mathbf{D}_\mathrm{f}^{(1)}\, \boldsymbol{\varepsilon}(\mathbf{u}_\mathrm{f}) + \widetilde{\mathbf{D}}_\mathrm{f}^{(2)}(\omega)\, \boldsymbol{\varepsilon}(\mathbf{u}_\mathrm{f}) \tag{8b}$$

with:

$$\begin{aligned}
\mathbf{D}_\mathrm{s}^{(1)} &= \left(\lambda + \frac{(1-\phi)^2}{\phi} P_0\right) \mathbf{D} + \mu\, \mathbf{diag}\begin{pmatrix}2 & 2 & 2 & 1 & 1 & 1\end{pmatrix} \\
\mathbf{D}_\mathrm{sf}^{(1)} &= (1-\phi)\, P_0\, \mathbf{D} \\
\mathbf{D}_\mathrm{f}^{(1)} &= \phi\, P_0\, \mathbf{D} \\
\widetilde{\mathbf{D}}_\mathrm{s}^{(2)}(\omega) &= \left(\widetilde{K}_\mathrm{f} - P_0\right) \mathbf{D}_\mathrm{s}^{(2)} = \frac{(1-\phi)^2}{\phi} \left(\widetilde{K}_\mathrm{f} - P_0\right) \mathbf{D} \\
\widetilde{\mathbf{D}}_\mathrm{sf}^{(2)}(\omega) &= \left(\widetilde{K}_\mathrm{f} - P_0\right) \mathbf{D}_\mathrm{sf}^{(2)} = (1-\phi) \left(\widetilde{K}_\mathrm{f} - P_0\right) \mathbf{D} \\
\widetilde{\mathbf{D}}_\mathrm{f}^{(2)}(\omega) &= \left(\widetilde{K}_\mathrm{f} - P_0\right) \mathbf{D}_\mathrm{f}^{(2)} = \phi \left(\widetilde{K}_\mathrm{f} - P_0\right) \mathbf{D}
\end{aligned} \qquad \text{where } \mathbf{D} = \begin{bmatrix}
1 & 1 & 1 & 0 & 0 & 0 \\
1 & 1 & 1 & 0 & 0 & 0 \\
1 & 1 & 1 & 0 & 0 & 0 \\
0 & 0 & 0 & 0 & 0 & 0 \\
0 & 0 & 0 & 0 & 0 & 0 \\
0 & 0 & 0 & 0 & 0 & 0
\end{bmatrix}$$

In this contribution, the Lamé parameters for the solid frame are considered real and frequency-independent, so that no structural damping is taken into account in the porous media behaviour. However, the method presented is also valid and straightforward to establish when structural damping is taken into account.

2.2 Fluid-structure interaction problem

In this subsection, boundary and coupling conditions are recalled for the poro-acoustic coupled problem presented in Fig. 1, in order to establish the discretized FE problem.

2.2.1 Poro-acoustic coupling and boundary conditions

At external boundary of the acoustic fluid domain, rigid cavity conditions are classically imposed by setting a free pressure field ($\partial_1\Omega_\mathrm{F} = \{\emptyset\}$). A harmonic excitation is prescribed via an acoustic source:

$$\mathbf{grad}\, p \cdot \mathbf{n} = \omega^2 \rho_\mathrm{F}\, u_\mathrm{Fb} \quad \text{on } \partial_2\Omega_\mathrm{F} \tag{9}$$

where u_Fb is set to zero out of the acoustic source included in $\partial_2\Omega_\mathrm{F}$.

Coupling at interface Γ_FP is given by normal stress and normal displacement continuity conditions between acoustic fluid and both fluid and solid phases of porous media:

$$\boldsymbol{\sigma}_\mathrm{s}\, \mathbf{n} + (1-\phi)\, p\, \mathbf{n} = \mathbf{0} \quad \text{on } \Gamma_\mathrm{FP} \tag{10a}$$

$$\boldsymbol{\sigma}_\mathrm{f}\, \mathbf{n} + \phi\, p\, \mathbf{n} = \mathbf{0} \quad \text{on } \Gamma_\mathrm{FP} \tag{10b}$$

$$\mathbf{u}_\mathrm{F} \cdot \mathbf{n} - (1-\phi)\mathbf{u}_\mathrm{s} \cdot \mathbf{n} - \phi \mathbf{u}_\mathrm{f} \cdot \mathbf{n} = 0 \quad \text{on } \Gamma_\mathrm{FP} \tag{11}$$

where ϕ is the porosity of the porous material, i.e. the volume fraction of fluid.

No external force is applied to the outer boundary of the porous media beside at interface Γ_FP. Therefore, $\partial_2\Omega_\mathrm{P} = \{\emptyset\}$ in the considered problem. Finally, at external boundary $\partial_1\Omega_\mathrm{P}$, two types of boundary conditions can be prescribed, the porous material being considered either as sliding or bounded to a rigid wall (Table 2).

Bounded layer	***Sliding layer***
$\mathbf{u}_\mathrm{s} = \mathbf{0}$	$\mathbf{u}_\mathrm{s} \cdot \mathbf{n}_\mathrm{P} = 0$
$\mathbf{u}_\mathrm{f} \cdot \mathbf{n}_\mathrm{P} = 0$	$\mathbf{u}_\mathrm{f} \cdot \mathbf{n}_\mathrm{P} = 0$

Table 2: Boundary conditions for porous layer on $\partial_1\Omega_\mathrm{P}$

2.2.2 Finite element discretized problem

The test-function method is used to derive the variational formulation of the coupled problem. For this purpose, the spaces of sufficiently smooth functions C_p, $C_{\mathbf{u}_\mathrm{s}}$ and $C_{\mathbf{u}_\mathrm{f}}$ are introduced, associated to the field variables p, $\mathbf{u}_\mathrm{s}$ and $\mathbf{u}_\mathrm{f}$ respectively. Let δp, $\delta\mathbf{u}_\mathrm{s}$, $\delta\mathbf{u}_\mathrm{f}$ be the frequency-independent test functions, associated to p, $\mathbf{u}_\mathrm{s}$, $\mathbf{u}_\mathrm{f}$ respectively, and belonging to their respective admissible spaces C_p, $C^*_{\mathbf{u}_\mathrm{s}} = \{\delta\mathbf{u}_\mathrm{s} \in C_{\mathbf{u}_\mathrm{s}} | \delta\mathbf{u}_\mathrm{s} = \mathbf{0} \quad \text{on } \partial_1\Omega_\mathrm{P}\}$, and $C^*_{\mathbf{u}_\mathrm{f}} = \{\delta\mathbf{u}_\mathrm{f} \in C_{\mathbf{u}_\mathrm{f}} | \delta\mathbf{u}_\mathrm{f} = \mathbf{0} \quad \text{on } \partial_1\Omega_\mathrm{P}\}$.

Equations (1), (9), and (11) lead to:

$$\begin{aligned}\int_{\Omega_\mathrm{F}} \mathbf{grad} p \,.\mathbf{grad}\delta p \,\mathrm{d}V - \frac{\omega^2}{c_0^2}\int_{\Omega_\mathrm{F}} p\,\delta p \,\mathrm{d}V - \omega^2\rho_\mathrm{F}(1-\phi)\int_{\Gamma_\mathrm{FP}} \mathbf{u}_\mathrm{s}.\mathbf{n}\,\delta p\,\mathrm{d}\Sigma \\ -\omega^2\rho_\mathrm{F}\phi\int_{\Gamma_\mathrm{FP}} \mathbf{u}_\mathrm{f}.\mathbf{n}\,\delta p\,\mathrm{d}\Sigma = \omega^2\rho_\mathrm{F}\int_{\partial_2\Omega_\mathrm{F}} u_\mathrm{Fb}\,\delta p\,\mathrm{d}\Sigma\end{aligned} \tag{12}$$

Equations (2a), (8a),and (10a) lead to:

$$\begin{aligned}
&\int_{\Omega_\mathrm{P}} \mathrm{tr}\left[\mathbf{D}_\mathrm{s}^{(1)}\,\boldsymbol{\varepsilon}(\mathbf{u}_\mathrm{s})\,\boldsymbol{\varepsilon}(\delta\mathbf{u}_\mathrm{s})\right]\,\mathrm{d}V + \int_{\Omega_\mathrm{P}} \mathrm{tr}\left[\mathbf{D}_\mathrm{sf}^{(1)}\,\boldsymbol{\varepsilon}(\mathbf{u}_\mathrm{f})\,\boldsymbol{\varepsilon}(\delta\mathbf{u}_\mathrm{s})\right]\,\mathrm{d}V \\
&+\left(\widetilde{K}_\mathrm{f}-P_0\right)\left[\int_{\Omega_\mathrm{P}} \mathrm{tr}\left[\mathbf{D}_\mathrm{s}^{(2)}\,\boldsymbol{\varepsilon}(\mathbf{u}_\mathrm{s})\,\boldsymbol{\varepsilon}(\delta\mathbf{u}_\mathrm{s})\right]\,\mathrm{d}V + \int_{\Omega_\mathrm{P}} \mathrm{tr}\left[\mathbf{D}_\mathrm{sf}^{(2)}\,\boldsymbol{\varepsilon}(\mathbf{u}_\mathrm{f})\,\boldsymbol{\varepsilon}(\delta\mathbf{u}_\mathrm{s})\right]\,\mathrm{d}V\right] \\
&+\mathrm{i}\,\omega\,\widetilde{b}\left[\int_{\Omega_\mathrm{P}} \mathbf{u}_\mathrm{s}.\delta\mathbf{u}_\mathrm{s}\,\mathrm{d}V - \int_{\Omega_\mathrm{P}} \mathbf{u}_\mathrm{f}.\delta\mathbf{u}_\mathrm{s}\,\mathrm{d}V\right] \\
&-\omega^2\left[\int_{\Omega_\mathrm{P}} (\rho_\mathrm{s}+\rho_\mathrm{a})\,\mathbf{u}_\mathrm{s}.\delta\mathbf{u}_\mathrm{s}\,\mathrm{d}V - \int_{\Omega_\mathrm{P}} \rho_\mathrm{a}\mathbf{u}_\mathrm{f}.\delta\mathbf{u}_\mathrm{s}\,\mathrm{d}V\right] - (1-\phi)\int_{\Gamma_\mathrm{FP}} p\,\mathbf{n}.\delta\mathbf{u}_\mathrm{s}\,\mathrm{d}\Sigma = 0
\end{aligned} \tag{13}$$

Equations (2b), (8b),and (10b) lead to:

$$\begin{aligned}
&\int_{\Omega_\mathrm{P}} \mathrm{tr}\left[\mathbf{D}_\mathrm{f}^{(1)}\,\boldsymbol{\varepsilon}(\mathbf{u}_\mathrm{f})\,\boldsymbol{\varepsilon}(\delta\mathbf{u}_\mathrm{f})\right]\,\mathrm{d}V + \int_{\Omega_\mathrm{P}} \mathrm{tr}\left[\mathbf{D}_\mathrm{sf}^{(1)}\,\boldsymbol{\varepsilon}(\mathbf{u}_\mathrm{s})\,\boldsymbol{\varepsilon}(\delta\mathbf{u}_\mathrm{f})\right]\,\mathrm{d}V \\
&+\left(\widetilde{K}_\mathrm{f}-P_0\right)\left[\int_{\Omega_\mathrm{P}} \mathrm{tr}\left[\mathbf{D}_\mathrm{f}^{(2)}\,\boldsymbol{\varepsilon}(\mathbf{u}_\mathrm{f})\,\boldsymbol{\varepsilon}(\delta\mathbf{u}_\mathrm{f})\right]\,\mathrm{d}V + \int_{\Omega_\mathrm{P}} \mathrm{tr}\left[\mathbf{D}_\mathrm{sf}^{(2)}\,\boldsymbol{\varepsilon}(\mathbf{u}_\mathrm{s})\,\boldsymbol{\varepsilon}(\delta\mathbf{u}_\mathrm{f})\right]\,\mathrm{d}V\right] \\
&+\mathrm{i}\,\omega\,\widetilde{b}\left[\int_{\Omega_\mathrm{P}} \mathbf{u}_\mathrm{f}.\delta\mathbf{u}_\mathrm{f}\,\mathrm{d}V - \int_{\Omega_\mathrm{P}} \mathbf{u}_\mathrm{s}.\delta\mathbf{u}_\mathrm{f}\,\mathrm{d}V\right] \\
&-\omega^2\left[\int_{\Omega_\mathrm{P}} (\phi\rho_\mathrm{f}+\rho_\mathrm{a})\,\mathbf{u}_\mathrm{f}.\delta\mathbf{u}_\mathrm{f}\,\mathrm{d}V - \int_{\Omega_\mathrm{P}} \rho_\mathrm{a}\mathbf{u}_\mathrm{s}.\delta\mathbf{u}_\mathrm{f}\,\mathrm{d}V\right] - \phi\int_{\Gamma_\mathrm{FP}} p\,\mathbf{n}.\delta\mathbf{u}_\mathrm{f}\,\mathrm{d}\Sigma = 0
\end{aligned} \tag{14}$$

After discretization of the various terms in Eqs. (12)-(14) by the FE method and dividing Eq. (12) by ρ_F, the following matrix equation for the coupled problem is obtained:

$$\begin{aligned}
&\left(\begin{bmatrix} \mathbf{K}_\mathrm{F} & \mathbf{0} & \mathbf{0} \\ -(1-\phi)\mathbf{A}_\mathrm{Fs}^T & \mathbf{K}_\mathrm{ss}^{(1)} & \mathbf{K}_\mathrm{sf}^{(1)} \\ -\phi\mathbf{A}_\mathrm{Ff}^T & \mathbf{K}_\mathrm{sf}^{(1)T} & \mathbf{K}_\mathrm{ff}^{(1)} \end{bmatrix} + \left(\widetilde{K}_\mathrm{f}-P_0\right)\begin{bmatrix} \mathbf{0} & \mathbf{0} & \mathbf{0} \\ \mathbf{0} & \mathbf{K}_\mathrm{ss}^{(2)} & \mathbf{K}_\mathrm{sf}^{(2)} \\ \mathbf{0} & \mathbf{K}_\mathrm{sf}^{(2)T} & \mathbf{K}_\mathrm{ff}^{(2)} \end{bmatrix}\right. \\
&\left.+\mathrm{i}\,\omega\,\widetilde{b}\begin{bmatrix} \mathbf{0} & \mathbf{0} & \mathbf{0} \\ \mathbf{0} & \mathbf{C}_\mathrm{ss} & \mathbf{C}_\mathrm{sf} \\ \mathbf{0} & \mathbf{C}_\mathrm{sf}^T & \mathbf{C}_\mathrm{ff} \end{bmatrix} - \omega^2\begin{bmatrix} \mathbf{M}_\mathrm{F} & (1-\phi)\mathbf{A}_\mathrm{Fs} & \phi\mathbf{A}_\mathrm{Ff} \\ \mathbf{0} & \mathbf{M}_\mathrm{ss} & \mathbf{M}_\mathrm{sf} \\ \mathbf{0} & \mathbf{M}_\mathrm{sf}^T & \mathbf{M}_\mathrm{ff} \end{bmatrix}\right)\begin{bmatrix} \mathbf{P} \\ \mathbf{U}_\mathrm{s} \\ \mathbf{U}_\mathrm{f} \end{bmatrix} = \begin{bmatrix} \omega^2\mathbf{U}_\mathrm{Fb} \\ \mathbf{0} \\ \mathbf{0} \end{bmatrix}
\end{aligned} \tag{15}$$

This non-symmetric formulation can be symmetrized for a resolution in the frequency domain by dividing the acoustic equation by ω^2 ($\omega \neq 0$). The interest of rewriting the porous media formulation into four matrices ($\mathbf{K}_\mathrm{ii}^{(1)}$, $\mathbf{K}_\mathrm{ii}^{(2)}$, $\mathbf{C}_\mathrm{ii}$, and $\mathbf{M}_\mathrm{ii}$) is already partly visible. In fact, it involves constant real-valued matrices which can be assembled once, while only the complex and frequency-dependent factors $\widetilde{K}_\mathrm{f}$ and $\widetilde{b}$ are recomputed at each frequency increment. In addition to that, the amount of memory used is the same as using two complex-valued and frequency-dependent matrices, as the sparsity is unchanged. More importantly, the main interest underlined in this work is the possibility to use such a formulation in the context of modal reduction techniques.

3 MODAL REDUCTION OF THE POROUS MEDIA

3.1 Presentation of the proposed solution strategy

The proposed reduction method is applied to the dissipative porous media of a poro-acoustic coupled problem, which is the costly part of the model. For the sake of conciseness, the case of a rigid acoustic cavity with a single porous layer on one wall is considered. Notations used are presented in Fig. 2.

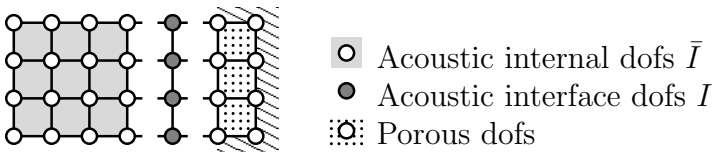

Figure 2: Problem description for modal reduction of porous media

The acoustic degrees of freedom (dofs) are separated into internal ones (subscript $\bar{I}$), and those at interface with the porous media (subscript I). These notations allow easy extension of the method to problems with multiple interfaces [10]. The coupled porous media matrices are now considered, involving four matrices $\mathbf{K}_{\mathrm{P}}^{(1)}$, $\mathbf{K}_{\mathrm{P}}^{(2)}$, $\mathbf{C}_{\mathrm{P}}$, and $\mathbf{M}_{\mathrm{P}}$ corresponding to the set of unknowns $\mathbf{U}_{\mathrm{P}}$ such that, for each matrix indexed by P, i.e. $\mathbf{B}_{\mathrm{P}} \in \{\mathbf{K}_{\mathrm{P}}^{(1)}, \mathbf{K}_{\mathrm{P}}^{(2)}, \mathbf{C}_{\mathrm{P}}, \mathbf{M}_{\mathrm{P}}\}$:

$$\mathbf{B}_{\mathrm{P}} = \begin{bmatrix} \mathbf{B}_{\mathrm{ss}} & \mathbf{B}_{\mathrm{sf}} \\ \mathbf{B}_{\mathrm{sf}} & \mathbf{B}_{\mathrm{ff}} \end{bmatrix} \quad \text{and} \quad \mathbf{U}_{\mathrm{P}} = \begin{bmatrix} \mathbf{U}_{\mathrm{s}} \\ \mathbf{U}_{\mathrm{f}} \end{bmatrix} \tag{16}$$

Similarly, the coupling between the interface acoustic dofs (subscript I) and the porous dofs (subscript P) is denoted:

$$\mathbf{A}_{I\mathrm{P}} = \begin{bmatrix} (1-\phi)\mathbf{A}_{I\mathrm{s}} & \phi\mathbf{A}_{I\mathrm{f}} \end{bmatrix} \tag{17}$$

Consequently, for modal reduction purposes, matrix set of equations (15) can be written:

$$\begin{bmatrix} \mathbf{K}_{\bar{I}\bar{I}} - \omega^2\mathbf{M}_{\bar{I}\bar{I}} & \mathbf{K}_{\bar{I}I} - \omega^2\mathbf{M}_{\bar{I}I} & \mathbf{0} \\ \mathbf{K}_{I\bar{I}} - \omega^2\mathbf{M}_{I\bar{I}} & \mathbf{K}_{II} - \omega^2\mathbf{M}_{II} & -\omega^2\mathbf{A}_{I\mathrm{P}} \\ \mathbf{0} & -{\mathbf{A}_{I\mathrm{P}}}^T & \mathbf{K}_{\mathrm{P}}^{(1)} + \left(\widetilde{K}_{\mathrm{f}} - P_0\right)\mathbf{K}_{\mathrm{P}}^{(2)} + \mathrm{i}\,\omega\,\widetilde{b}\mathbf{C}_{\mathrm{P}} - \omega^2\mathbf{M}_{\mathrm{P}} \end{bmatrix} \begin{bmatrix} \mathbf{P}_{\bar{I}} \\ \mathbf{P}_I \\ \mathbf{U}_{\mathrm{P}} \end{bmatrix} = \begin{bmatrix} \omega^2\mathbf{U}_{\bar{I}\mathrm{b}} \\ \mathbf{0} \\ \mathbf{0} \end{bmatrix} \tag{18}$$

and can be symmetrized by dividing the acoustic equations (lines 1 and 2) by ω^2 ($\omega \neq 0$).

3.2 Modal reduction

From the proposed expression of the porous media FE problem, real-valued normal modes can be computed associated to the conservative poroelastic eigenvalue problem:

$$\left(\mathbf{K}_{\mathrm{P}}^{(1)} - \omega^2\mathbf{M}_{\mathrm{P}}\right)\boldsymbol{\phi} = \mathbf{0} \tag{19}$$

It is supposed that the Dirichlet boundary conditions imposed to the porous media result in a nonsingular $\mathbf{K}_{\mathrm{P}}^{(1)}$ matrix, therefore removing zero-frequency modes. A modal reduction basis $\mathbf{\Phi}_{\mathrm{P}m}$ is built, selecting m low frequency modes. They are normalized with respect to the porous mass matrix $\mathbf{M}_{\mathrm{P}}$ so that:

$$\mathbf{\Phi}_{\mathrm{P}m}{}^T \mathbf{M}_{\mathrm{P}} \mathbf{\Phi}_{\mathrm{P}m} = \mathbf{I}_m \tag{20a}$$

$$\mathbf{\Phi}_{\mathrm{P}m}{}^T \mathbf{K}_{\mathrm{P}}^{(1)} \mathbf{\Phi}_{\mathrm{P}m} = \mathbf{\Omega}_m \tag{20b}$$

where $\mathbf{I}_m$ is a unit matrix of dimension m, and $\mathbf{\Omega}_m$ a diagonal matrix of same size, with the m lowest eigenvalues of (19) on its diagonal.

There are two key points that make a reduction method computationally efficient, which are its ability to:

- converge rapidly to the expected solution when adding modes in the basis, thus allowing a subsequent reduction in the number of dofs, as well as a reasonable time allocated to the computation of the modes,
- preserve or improve the sparsity of the matrices after projection, and ideally produce diagonal submatrices.

The former aspect will be examined on an example in Section 4. Regarding the second aspect, the sparsity of matrices $\mathbf{K}_{\mathrm{P}}^{(2)}$ and $\mathbf{C}_{\mathrm{P}}$ after projection on the modal basis is fundamental to take advantage of the diagonal form of projected $\mathbf{K}_{\mathrm{P}}^{(1)}$ and $\mathbf{M}_{\mathrm{P}}$. The choices made for the discretization of porous media, among which the separation of the "static" and "dynamic" parts of the effective bulk modulus, seem to fulfill this requirement. In fact, as will be shown in Section 4, it results in sparse reduced $\mathbf{K}_{\mathrm{P}}^{(2)}$ and $\mathbf{C}_{\mathrm{P}}$, and even orthogonality of some modes with respect to these matrices. Therefore, after testing the m retained modes for their orthogonal properties with respect to $\mathbf{K}_{\mathrm{P}}^{(2)}$ and $\mathbf{C}_{\mathrm{P}}$, they are separated into o "orthogonal" ($\mathbf{\Phi}_{\mathrm{P}o}$) and n "non-orthogonal" ($\mathbf{\Phi}_{\mathrm{P}n}$) ones, so that:

$$\begin{bmatrix}\mathbf{\Phi}_{\mathrm{P}n} & \mathbf{\Phi}_{\mathrm{P}o}\end{bmatrix}^T \mathbf{M}_{\mathrm{P}} \begin{bmatrix}\mathbf{\Phi}_{\mathrm{P}n} & \mathbf{\Phi}_{\mathrm{P}o}\end{bmatrix} = \begin{bmatrix}\mathbf{I}_n & \mathbf{0} \\ \mathbf{0} & \mathbf{I}_o\end{bmatrix} \tag{21a}$$

$$\begin{bmatrix}\mathbf{\Phi}_{\mathrm{P}n} & \mathbf{\Phi}_{\mathrm{P}o}\end{bmatrix}^T \mathbf{K}_{\mathrm{P}}^{(1)} \begin{bmatrix}\mathbf{\Phi}_{\mathrm{P}n} & \mathbf{\Phi}_{\mathrm{P}o}\end{bmatrix} = \begin{bmatrix}\mathbf{\Omega}_n & \mathbf{0} \\ \mathbf{0} & \mathbf{\Omega}_o\end{bmatrix} \tag{21b}$$

$$\begin{bmatrix}\mathbf{\Phi}_{\mathrm{P}n} & \mathbf{\Phi}_{\mathrm{P}o}\end{bmatrix}^T \mathbf{K}_{\mathrm{P}}^{(2)} \begin{bmatrix}\mathbf{\Phi}_{\mathrm{P}n} & \mathbf{\Phi}_{\mathrm{P}o}\end{bmatrix} = \begin{bmatrix}\boldsymbol{\kappa}_n & \mathbf{0} \\ \mathbf{0} & \boldsymbol{\kappa}_o\end{bmatrix} \tag{21c}$$

$$\begin{bmatrix}\mathbf{\Phi}_{\mathrm{P}n} & \mathbf{\Phi}_{\mathrm{P}o}\end{bmatrix}^T \mathbf{C}_{\mathrm{P}} \begin{bmatrix}\mathbf{\Phi}_{\mathrm{P}n} & \mathbf{\Phi}_{\mathrm{P}o}\end{bmatrix} = \begin{bmatrix}\boldsymbol{\zeta}_n & \mathbf{0} \\ \mathbf{0} & \boldsymbol{\zeta}_o\end{bmatrix} \tag{21d}$$

where $\mathbf{I}_n$, $\mathbf{\Omega}_n$ and $\mathbf{I}_o$, $\mathbf{\Omega}_o$, $\boldsymbol{\kappa}_o$, $\boldsymbol{\zeta}_o$ are diagonal matrices of respective dimensions n and o, while $\boldsymbol{\kappa}_n$ and $\boldsymbol{\zeta}_n$ are non-diagonal sparse square matrices of dimension n.

There are several options for the choice of attachment functions, but in this work, the single degree of freedom (dof) per node associated to the acoustic domain is put

to advantage. Attachment functions are computed as the $\mathbf{K}_{\mathrm{P}}^{(1)}$– static responses of the porous media to unit pressure successively imposed at each interface acoustic dof:

$$\begin{bmatrix} -\mathbf{A}_{I\mathrm{P}}{}^T & \mathbf{K}_{\mathrm{P}}^{(1)} \end{bmatrix} \begin{bmatrix} \mathbf{I}_I \\ \mathbf{\Psi}_{\mathrm{P}I} \end{bmatrix} = \begin{bmatrix} \mathbf{0} \end{bmatrix} \Rightarrow \mathbf{\Psi}_{\mathrm{P}I} = \mathbf{K}_{\mathrm{P}}^{(1)^{-1}} \mathbf{A}_{I\mathrm{P}}{}^T \tag{22}$$

Again, assumption is made that $\mathbf{K}_{\mathrm{P}}^{(1)}$ is not singular. If otherwise, a shift in frequency using the mass matrix $\mathbf{M}_{\mathrm{P}}$ can be set instead, to define pseudo-static attachment functions, but is not considered in this work.

The corresponding change of basis, leaving acoustic dofs uncondensed, is then:

$$\begin{bmatrix} \mathbf{P}_{\bar{I}} \\ \mathbf{P}_I \\ \mathbf{U}_{\mathrm{P}} \end{bmatrix} = \begin{bmatrix} \mathbf{I}_{\bar{I}} & \mathbf{0} & \mathbf{0} & \mathbf{0} \\ \mathbf{0} & \mathbf{I}_I & \mathbf{0} & \mathbf{0} \\ \mathbf{0} & \mathbf{\Psi}_{\mathrm{P}I} & \mathbf{\Phi}_{\mathrm{P}n} & \mathbf{\Phi}_{\mathrm{P}o} \end{bmatrix} \begin{bmatrix} \mathbf{P}_{\bar{I}} \\ \mathbf{P}_I \\ \boldsymbol{\alpha}_n \\ \boldsymbol{\alpha}_o \end{bmatrix} \tag{23}$$

where $\boldsymbol{\alpha}_n$ and $\boldsymbol{\alpha}_o$ are the modal coordinates vectors associated to the selected "non-orthogonal" and "orthogonal" modes respectively.

Applying change of basis (23) to symmetrized Eq. (18) leads to the following reduced set of equations:

$$\begin{aligned} \Bigg(& \begin{bmatrix} \frac{1}{\omega^2}\mathbf{K}_{\bar{I}\bar{I}} - \mathbf{M}_{\bar{I}\bar{I}} & \frac{1}{\omega^2}\mathbf{K}_{\bar{I}I} - \mathbf{M}_{\bar{I}I} & \mathbf{0} & \mathbf{0} \\ \frac{1}{\omega^2}\mathbf{K}_{I\bar{I}} - \mathbf{M}_{I\bar{I}} & \frac{1}{\omega^2}\mathbf{K}_{II} - \mathbf{M}_{II} - \mathbf{K}_{\mathrm{P}_{II}}^{(1)} & \mathbf{0} & \mathbf{0} \\ \mathbf{0} & \mathbf{0} & \mathbf{\Omega}_n & \mathbf{0} \\ \mathbf{0} & \mathbf{0} & \mathbf{0} & \mathbf{\Omega}_o \end{bmatrix} + \left(\widetilde{K}_{\mathrm{f}} - P_0\right) \begin{bmatrix} \mathbf{0} & \mathbf{0} & \mathbf{0} & \mathbf{0} \\ \mathbf{0} & \mathbf{K}_{\mathrm{P}_{II}}^{(2)} & \mathbf{K}_{\mathrm{P}_{In}}^{(2)} & \mathbf{K}_{\mathrm{P}_{Io}}^{(2)} \\ \mathbf{0} & \mathbf{K}_{\mathrm{P}_{nI}}^{(2)} & \boldsymbol{\kappa}_n & \mathbf{0} \\ \mathbf{0} & \mathbf{K}_{\mathrm{P}_{oI}}^{(2)} & \mathbf{0} & \boldsymbol{\kappa}_o \end{bmatrix} \\ & + \mathrm{i}\,\omega\,\widetilde{b} \begin{bmatrix} \mathbf{0} & \mathbf{0} & \mathbf{0} & \mathbf{0} \\ \mathbf{0} & \mathbf{C}_{\mathrm{P}_{II}} & \mathbf{C}_{\mathrm{P}_{In}} & \mathbf{C}_{\mathrm{P}_{Io}} \\ \mathbf{0} & \mathbf{C}_{\mathrm{P}_{nI}} & \boldsymbol{\zeta}_n & \mathbf{0} \\ \mathbf{0} & \mathbf{C}_{\mathrm{P}_{oI}} & \mathbf{0} & \boldsymbol{\zeta}_o \end{bmatrix} - \omega^2 \begin{bmatrix} \mathbf{0} & \mathbf{0} & \mathbf{0} & \mathbf{0} \\ \mathbf{0} & \mathbf{M}_{\mathrm{P}_{II}} & \mathbf{M}_{\mathrm{P}_{In}} & \mathbf{M}_{\mathrm{P}_{Io}} \\ \mathbf{0} & \mathbf{M}_{\mathrm{P}_{nI}} & \mathbf{I}_n & \mathbf{0} \\ \mathbf{0} & \mathbf{M}_{\mathrm{P}_{oI}} & \mathbf{0} & \mathbf{I}_o \end{bmatrix} \Bigg) \begin{bmatrix} \mathbf{P}_{\bar{I}} \\ \mathbf{P}_I \\ \boldsymbol{\alpha}_n \\ \boldsymbol{\alpha}_o \end{bmatrix} = \begin{bmatrix} \mathbf{U}_{\mathrm{Fb}} \\ \mathbf{0} \\ \mathbf{0} \\ \mathbf{0} \end{bmatrix} \end{aligned} \tag{24}$$

where for $\mathbf{B}_{\mathrm{P}} \in \{\mathbf{K}_{\mathrm{P}}^{(1)}, \mathbf{K}_{\mathrm{P}}^{(2)}, \mathbf{C}_{\mathrm{P}}, \mathbf{M}_{\mathrm{P}}\}$:

$$\begin{aligned} \mathbf{B}_{\mathrm{P}_{II}} &= \mathbf{\Psi}_{\mathrm{P}I}^T \mathbf{B}_{\mathrm{P}} \mathbf{\Psi}_{\mathrm{P}I} \\ \mathbf{B}_{\mathrm{P}_{In}} &= \mathbf{\Psi}_{\mathrm{P}I}^T \mathbf{B}_{\mathrm{P}} \mathbf{\Phi}_{\mathrm{P}n} &= \mathbf{B}_{\mathrm{P}_{nI}}^T \\ \mathbf{B}_{\mathrm{P}_{Io}} &= \mathbf{\Psi}_{\mathrm{P}I}^T \mathbf{B}_{\mathrm{P}} \mathbf{\Phi}_{\mathrm{P}o} &= \mathbf{B}_{\mathrm{P}_{oI}}^T \end{aligned}$$

This reduction can be further improved using dynamic condensation of the "orthogonal" modal coordinates, which is rather straightforward, and not presented in this contribution.

4 APPLICATION AND RESULTS

The proposed reduction of porous media is tested on a dissipative poro-acoustic example initially proposed in [6]. It consists of a 3D hexahedric acoustic cavity of dimensions $0.4 \times 0.6 \times 0.75$ m^3 (see Fig. 3), with rigid walls, and filled with air. One wall is covered with a 5 cm-thick porous layer. The low frequency behaviour is tested applying a harmonic volume velocity source (Eq. (9)) at a corner of the cavity opposite the layer.

Frame	***Fluid***	***Porous***
	$c_0 = 343$ m/s	$\phi = 0.96$
$\lambda = 905357$ Pa	$\gamma = 1.4$	$\sigma = 32$ kNs/m^4
$\mu = 264062$ Pa	$Pr = 0.71$	$\alpha_\infty = 1.7$
$\rho_\mathrm{s} = 30$ kg/m^3	$\rho_\mathrm{f} = 1.21$ kg/m^3	$\Lambda = 90\ \mu$m
	$\eta = 1.84 \cdot 10^{-5}$ Ns/m^2	$\Lambda' = 165\ \mu$m

Table 3: Air and porous material parameters

The cavity is discretized by a $8 \times 12 \times 15$ mesh of 8-node hexahedric elements with pressure as single degree of freedom per node. The porous material, described by the Biot-Allard theory, and which material parameters are given in Table 3, is discretized by a $8 \times 12 \times 5$ mesh of 8-node hexahedric elements (Fig. 3), with 6 dofs per node corresponding to the fluid and solid phase displacements. Sticking Dirichlet boundary conditions are applied to the porous foam face in contact with the covered wall, and sliding conditions are prescribed on the side faces (see Table 2). This leads to a FE model with 1872 acoustic dofs, and 3070 porous dofs.

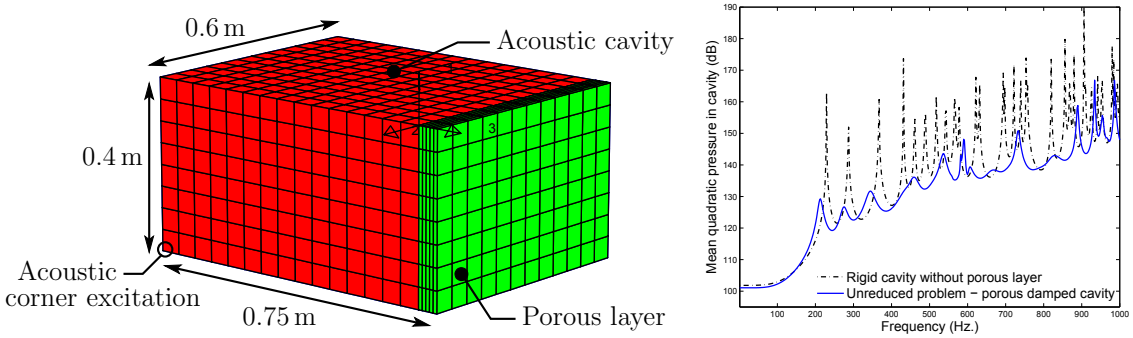

Figure 3: Acoustic cavity mesh and dimensions - Mean quadratic pressure reference FRF

The frequency response of the mean quadratic pressure in the acoustic cavity is given as an output (Fig. 3). The convergence is first checked, increasing the number of modes included in the basis, for a response in the range $[0 - 1000]$ Hz. Although many modes are needed in order to capture the dynamic behaviour of the porous media in the considered frequency range, the solution eventually converges toward the original solution (Fig. 4).

However, the interest of the proposed method specifically lies in the fact that real-valued modes are computed directly from the coupled porous problem, leading to good sparsity properties, as illustrated in Fig. 5. Thus, the 3070 porous media dofs are downsized to 800 modal unknowns, of which 414 correspond to $\mathbf{K}_\mathrm{P}^{(2)}$- and $\mathbf{C}_\mathrm{P}$-orthogonal modes, as introduced in Subsection 3.2. The sparsity is mostly affected by the use of attachment functions which fully couple interface dofs to modal unknowns. From a storage perspective, using $\mathbf{K}_\mathrm{P}^{(1)}$–static response for attachment function leads to uncoupled interface and modal unknowns in the reduction of $\mathbf{K}_\mathrm{P}^{(1)}$ (See Eq. 24).

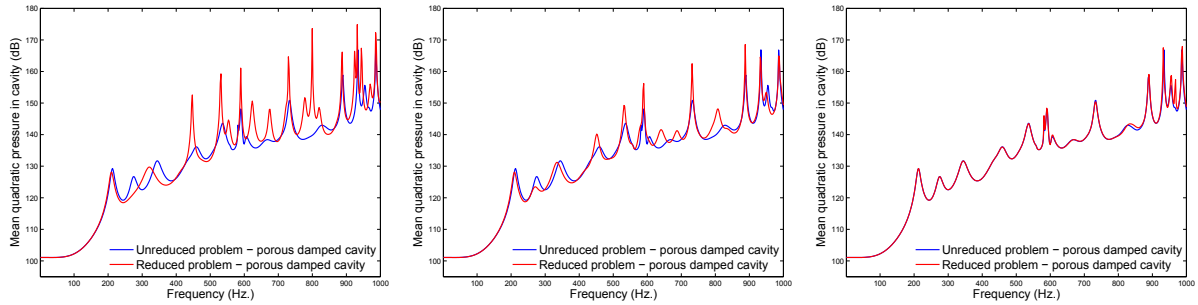

Figure 4: Mean quadratic pressure FRF. Convergence of the reduction: 100, 500, 800 modes

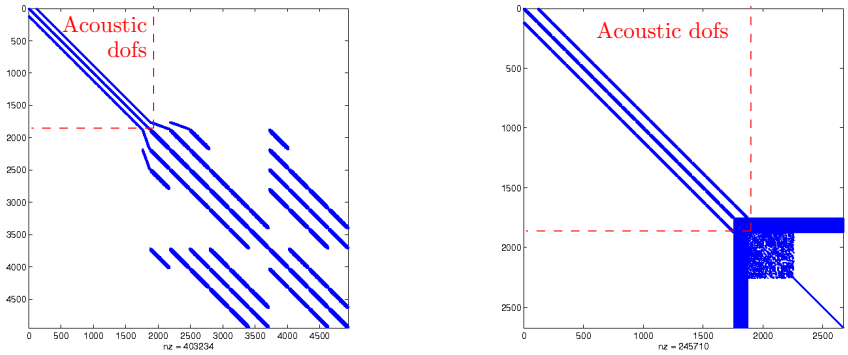

Figure 5: Sparsity of the system matrix for unreduced and reduced porous media

Regarding the computation time, a reduction including 800 modes in the basis leads to a factor 2.6 to 3.5 for the CPU time (Fig. 6), with 500 increments computed, depending whether the offset due to modes computation is taken into account or not.

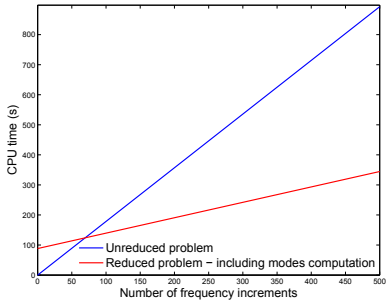

Figure 6: CPU time comparison for FRF computation

5 CONCLUSION

In this communication, the variational formulation of a harmonic poro-acoustic problem was presented. In order to improve the computational efficiency of the FE model, a modal-

based reduction of the poroelastic material was proposed, and tested on a rigid cavity treated with a porous layer. On this test application, the porous dofs were downsized from 3070 to 800 dofs, thus downsizing the coupled problem from 4942 to 2672 dofs, while preserving good sparsity properties. The computation time is therefore greatly improved. Regarding accuracy, the reduced model showed excellent match with the original problem up to 800 Hz, and good approximation up to 1000 Hz. This method can be easily combined with a similar reduction for the acoustic part evaluated by the authors [10]. Ongoing works are focusing on improvements for faster convergence to a good approximation of the original solution, as well as predictive criterion for modal truncation of the basis.

References

[1] J. F. Allard. *Sound propagation in porous media: modelling sound absorbing materials*. Elsevier, London, 1993.

[2] N. Atalla, M. A. Hamdi, and R. Panneton. Enhanced weak integral formulation for the mixed (u,p) poroelastic equations. *The Journal of the Acoustical Society of America*, 109(6):3065–3068, 2001.

[3] N. E Hörlin, M. Nordström, and P. Göransson. A 3-D hierarchical FE formulation of biot's equations for elasto-acoustic modelling of porous media. *Journal of Sound and Vibration*, 245(4):633–652, 2001.

[4] A. Bermúdez, L. Hervella-Nieto, and R. Rodríguez. Finite element computation of the vibrations of a plate-fluid system with interface damping. *Computer Methods in Applied Mechanics and Engineering*, 190(24-25):3021–3038, 2001.

[5] J. F Deü, W. Larbi, and R. Ohayon. Vibration and transient response of structural-acoustic interior coupled systems with dissipative interface. *Computer Methods in Applied Mechanics and Engineering*, 197(51-52):4894–4905, 2008.

[6] P. Davidsson and G. Sandberg. A reduction method for structure-acoustic and poroelastic-acoustic problems using interface-dependent lanczos vectors. *Computer Methods in Applied Mechanics and Engineering*, 195(17-18):1933–1945, 2006.

[7] C. Batifol, M. N. Ichchou, and M. A. Galland. Hybrid modal reduction for poroelastic materials. *Comptes Rendus Mécanique*, 336(10):757–765, 2008.

[8] O. Dazel, B. Brouard, N. Dauchez, A. Geslain, and C. H Lamarque. A free interface CMS technique to the resolution of coupled problem involving porous materials, application to a monodimensional problem. *Acta Acustica united with Acustica*, 96(2):247–257, 2010.

[9] H. J.-P. Morand and R. Ohayon. *Fluid Structure Interaction*. Wiley, 1995.

[10] R. Rumpler, A. Legay, and J. F Deü. Performance of a restrained-interface substructuring FE model for reduction of structural-acoustic problems with poroelastic damping. *Manuscript submitted for publication*.